Diurnal Variation of MCSs over Asia and the Western Pacific Region

SHU Yu[1,2] (束 宇), PAN Yinong[2*] (潘益农), and WANG Jinxin[2] (王金鑫)

1 *Nanjing Meteorology Bureau, Nanjing* 210019

2 *Key Laboratory of Mesoscale Severe Weather/Ministry of Education, and School of Atmospheric Sciences, Nanjing University, Nanjing* 210093

(Received October 11, 2012; in final form March 6, 2013)

ABSTRACT

Mesoscale convective systems (MCSs) are severe disaster-producing weather systems. Radar data and infrared satellite image are useful tools in MCS surveillance. The previous method of MCS census is to look through the printed infrared imagery manually. This method is not only subjective and inaccurate, but also inefficient. Different from previous studies, a new automatic MCS identification (AMI) method, which overcomes the above disadvantages, is used in the present study. The AMI method takes three steps: searching potential MCS profiles, tracking the MCS, and assessing the MCS, so as to capture MCSs from infrared satellite images. Finally, 47468 MCSs are identified over Asia and the western Pacific region during the warm seasons (May–October) from 1995 to 2008.

From this database, the geographical distribution and diurnal variation of MCSs are analyzed. The results show that different types of MCSs have similar geographical distributions. Latitude is the main control factor for MCS distribution. MCSs are most frequent over the central Tibetan Plateau; meanwhile, this area also has the highest hail frequency according to previous studies. Further, it is found that the diurnal variation of MCSs has little to do with MCSs' size or shape; MCSs in different areas have their own particular diurnal variation patterns. Based on the diurnal variation characteristics, MCSs are classified into four categories: the whole-day occurring MCSs in low latitude, the whole-day occurring MCSs in high latitude, the nocturnal MCSs, and the postmeridian MCSs. MCSs over most places of mainland China are postmeridian; but MCSs over the Sichuan basin and its vicinity are nocturnal. This conclusion is coincidental with the hail climatology of China.

Key words: mesoscale convective system, automatic MCS identification method, diurnal variation

Citation: Shu Yu, Pan Yinong, and Wang Jinxin, 2013: Diurnal variation of MCSs over Asia and the western Pacific region. *Acta Meteor. Sinica*, **27**(3), 435–445, doi: 10.1007/s13351-013-0305-6.

1. Introduction

Mesoscale convective systems (MCSs) may produce heavy rains in a broad range (Fritsch et al., 1986; Rafiuddin et al., 2010; Romatschke and Houze, 2011a, b). In addition, they can cause other convective weather, such as tornado, hailstorm, gale, and lightning (Maddox et al., 1982; Houze et al., 1990; Romatschke and Houze, 2010). Due to their important impact, it is imperative to gain a deeper insight into these disastrous systems. Recently, infrared satellite image and radar data are the main tools for MCS statistics study.

By means of infrared satellite imagery, Maddox (1980) first classified a particular type of MCS, i.e., mesoscale convective complex (MCC). Augustine and Howard (1988, 1991) examined the MCCs over the United States during 1985–1987 and obtained basic understanding of MCC activities in North America. Laing and Fritsch (1993a, b), Velasco and Fritsch (1987), and Miller and Fritsch (1991) investigated MCC activities in the Indian subcontinent, Africa, south of 20°N of America, and West Pacific, respectively. Anderson and Arritt (1998) defined another large class of MCS, i.e., persistent elongated convective system (PECS), which has eccentricities between

Supported by the National (Key) Basic Research and Development (973) Program of China (2013CB430103), National Natural Science Foundation of China (40875028), and Forecaster Special Project Funded by the Jiangsu Meteorological Bureau (2012-8).

*Corresponding author: pyn@nju.edu.cn.

0.2 and 0.7, in contrast to the $\geqslant 0.7$ eccentricities of MCCs. Ma et al. (1997) termed two circular MCS categories: Meso-α Convective System (MαCS) and Meso-β Convective System (MβCS). Furthermore, they surveyed the MαCSs and MβCSs over China and its vicinity during 1993–1995 and studied the temporal and spatial variations of the MCSs. Jirak et al. (2003) classified MCSs over the United States during 1996–1998 into four categories by means of both satellite and radar data. Besides, based on the Tropical Rainfall Measuring Mission (TRMM) satellite data, Romatschke et al. (2010) studied the extreme convection in the South Asian region and pointed out that land convection and oceanic convection formed preferentially in the afternoon and the evening, respectively. Zheng et al. (2008) uncovered some diurnal cycle characteristics of MCSs over China.

The past studies have greatly enriched our knowledge of MCSs. However, due to the method used in the MCS census, these studies have some limitations. Most of previous MCS censuses were done manually. To find the potential MCS, researchers need to eyeball and examine every printed nephogram. This manual method is inefficient and time-consuming. As a result, previous studies are confined to either a relatively small time frame and limited space coverage or a particular type of MCSs. What is worse, subjectivity and inaccuracy are inevitably involved in the manual MCS identifying process. It is noteworthy that Zheng et al. (2008) developed an automatic method to study MCSs. They analyzed the local MCS activity frequency. If the cloud top temperature was lower than –52°C, the number of MCS activities in that place would increase by one. This improved method well overcomes the disadvantages of the manual identification method. But, it has its own disadvantages. First of all, it is hard to catch the whole lifecycle of MCSs, and difficult to judge if the identified system is an MCS or not, according to the MCS definition. Consequently, this method fails to classify MCSs into categories. Secondly, the method is unable to be applied in study of the lifecycle and movement of MCSs. Thirdly, since the cloud top temperature of many non-MCS systems such as tropical cyclones (TCs) and some upper cirrus are low enough to meet the MCS definition, they are included in the MCS dataset when identifying MCSs; thus, the final results are not so accurate.

The above disadvantages hinder the statistic study of MCSs, and make the comprehensive and accurate MCS climatology study scarce and urgent. Such a background motivates the present work, in which a new MCS identification method—automatic MCS identification (AMI) method is used to establish a MCS database. The AMI method (Shu and Pan, 2010) can greatly reduce the consumption of labor and time, and eliminate the subjectivity arising from the identifying process. Besides, the AMI method can catch the whole MCS lifecycle from formation to dissipation. Hence, identifying MCSs becomes efficient and accurate. In this paper, using the AMI method, four types of MCSs with different sizes and shapes are recognized over Asia and the western Pacific region (AWPR) during the warm seasons of 1995–2008. Furthermore, geographical distributions and diurnal cycles of the MCSs over AWPR are analyzed.

2. Definition, data, and method

2.1 Terminology and MCS classification

Similar to the study by Shu et al. (2012), the present study attempts to classify MCSs into four discrete categories (Table 1) according to their size and shape: Meso-α Circular Convective System (MαCCS), Meso-α Elongated Convective System (MαECS), Meso-β Circular Convective System (MβCCS), and Meso-β Elongated Convective System (MβECS). Following previous studies on MCCs and MCSs (Maddox, 1980; Ma et al., 1997; Jirak et al., 2003), –52°C is used to define the cold cloud shield. In Table 1, the 50000- and 30000-km^2 size criterions are adopted from Jirak's definitions of meso-α and meso-β systems, respectively. To accord with past MCS studies in China (Ma et al., 1997), 0.5 is chosen as the eccentricity criterion to distinguish circular from linear MCSs, although the classical MCC eccentricity criterion is 0.7. On the other hand, similar to conventional PECS definition (Anderson and Arritt, 1998), 0.2 is used to limit the lower bound of linear MCSs.

Table 1. Definitions of MCS categories based on satellite infrared image (Shu et al., 2012)

MCS category	Area size of cold cloud shield	Duration	Eccentricity (ε)
MαCCS	$\geqslant$ 50000 km^2	$\geqslant$ 3 h	$\varepsilon \geqslant 0.5$
MαECS	$\geqslant$ 50000 km^2	$\geqslant$ 3 h	$0.2 \leqslant \varepsilon < 0.5$
MβCCS	$\geqslant$ 30000 km^2, and maximum size $\geqslant$ 50000 km^2	$\geqslant$ 3 h	$\varepsilon \geqslant 0.5$
MβECS	$\geqslant$ 30000 km^2, and maximum size $\geqslant$ 50000 km^2	$\geqslant$ 3 h	$0.2 \leqslant \varepsilon < 0.5$

Note: –52°C is used to define the cold cloud shield. Duration denotes the time period when size condition is satisfied. Eccentricity is calculated at the time of maximum extent of each MCS category.

Besides, according to Parker and Johnson (2000), the typical time scale of MCSs is 3 h. Hence, in the present work, the duration criterion for all the MCSs is set at 3 h, while the duration criterion for MCCs and PECSs are at least 6 h. As a result, MαCCS and MαECS in Table 1 are different from classical definitions of MCC and PECS in both eccentricity and duration.

In the following, formation of MCS is defined as the time when the size criterion is firstly satisfied. Maturation is the time when the cold cloud shield reaches the maximum extent. Dissipation is the time when the size criterion is no longer satisfied. Based on previous MCS studies, the period May–October is chosen as the convective season of AWPR. Furthermore, the 14-yr period from 1995 to 2008 is selected to obtain a large sample of MCSs. During this period, any system that meets the MCS criteria in Table 1 and matures within the region 0°–70°N, 70°–160°E is recorded. This large spatial domain covers most parts of AWPR.

2.2 Data

In this study, we use geostationary satellite infrared data from May to October of 1995–2008. The satellite data are from three satellites: Geostationary Meteorological Satellite 5 (GMS5), Geostationary Operational Environment Satellite 9 (GOES9), and Multi-functional Transport Satellite 1R (MTSAT-1R). The temporal resolution of the data is 1 h. For the year 1995, the data from May to August are not available. Thus, the dataset spans for 80 months. The satellite infrared data have been interpolated onto a 0.05°×0.05° grid over the domain of interest (0°–70°N, 70°–160°E).

2.3 MCS identification method

In present study, we use the AMI method (Shu and Pan, 2010) to establish an MCS database. The AMI method takes three steps to capture MCS from satellite infrared data. The first step is to capture all the potential MCS profiles of each time. All the cloud clusters with temperature lower than –52°C are considered as potential MCS profiles. The second step is to track the potential MCS from its initial profile to its last profile. The third step is to assess if the system found in step 2 is an MCS or not according to Table 1. After the AMI process, we obtain a database consisting of systems that meet the definitions in Table 1. TCs can easily meet the definitions, and are unavoidably involved in the database. Therefore, we remove TCs from the MCS database according to TC annuals. This procedure is somewhat subjective, and the preceding squall lines in association with TCs are also removed from the MCS database. Since it is hard for the cirrus to meet the MCS definitions in Table 1, the cirrus is not considered.

Shu and Pan (2010) indicated that when identifying MCSs with the AMI method, the error rate of MCS number is lower than 2% after removing TCs, and the accuracy of capturing the whole MCS lifecycle could reach about 85%.

3. Geographical distribution

In this study, by means of the AMI processing, 47468 MCSs are found over AWPR during the warm seasons of 1995–2008. In fact, they consist of 9241 MαCCSs, 3981 MβCCSs, 25126 MαECSs, and 9120 MβECSs. Based on this MCS database, the geographical distribution and diurnal variation of MCSs are analyzed.

Geographical distributions of four different types of MCSs are plotted respectively (figure omitted). The results show that they have similar patterns, i.e., geographical distribution of MCSs has little to do with MCS size or shape. Hence, in the following, we just need to analyze the spatial distribution of the whole MCS database (Fig. 1). Figure 1 shows that latitude is the main control factor for MCS distribution. In AWPR, MCSs are mainly zonally distributed, with three zonations weakening from south to north.

The low latitude zone lies to the south of 25°N. High MCS frequency occurs over the Amindivi and Laccadive Islands, the Pakistan and Gangetic Plain, oceans in the east of the Bay of Bengal, the Strait of Malacca, the Indochina Peninsula, the South China Sea, and the Caroline Islands to the east of the Philippines. This active zone is mainly related to the intertropical convergence zone (ITCZ), which can provide strong lower troposphere convergence and upward motion (Lu and Duan, 2011). In addition, plentiful water vapor favors MCS activities in this zone (Roy et al., 2008). Furthermore, the low levels are always of high temperature and humidity, which results in strong convective instability in the low latitude zone.

The midlatitude zone lies between 25° and 38°N. The MCSs occur mainly over the north of the Indus Plain, the central and western parts of the Tibetan Plateau, the Hengduan Mountains, the Sichuan basin, East China, and oceans near the Ryukyu Islands. The MCSs in this zone are primarily related to the South Asian summer monsoon (SASM) and the East Asian summer monsoon (EASM). Shu and Pan (2012) analyzed the MCS geographical distribution by month, and pointed out that the SASM and EASM control the advance and retreat of the MCS active zone in mid and low latitudes. Besides, MCSs over the Tibetan Plateau are favored by the heating effect of the plateau.

The high latitude zone lies to the north of 38°N. MCSs are inactive in this zone because the summer monsoon could hardly reach this region. The comparatively active regions in this zone include the central part of the West Siberian Plain, Lake Balkhash and Lake Issyk-Kul areas, Sayan Mountains and Lake Baikal areas, and areas in the east of the Great Khin-

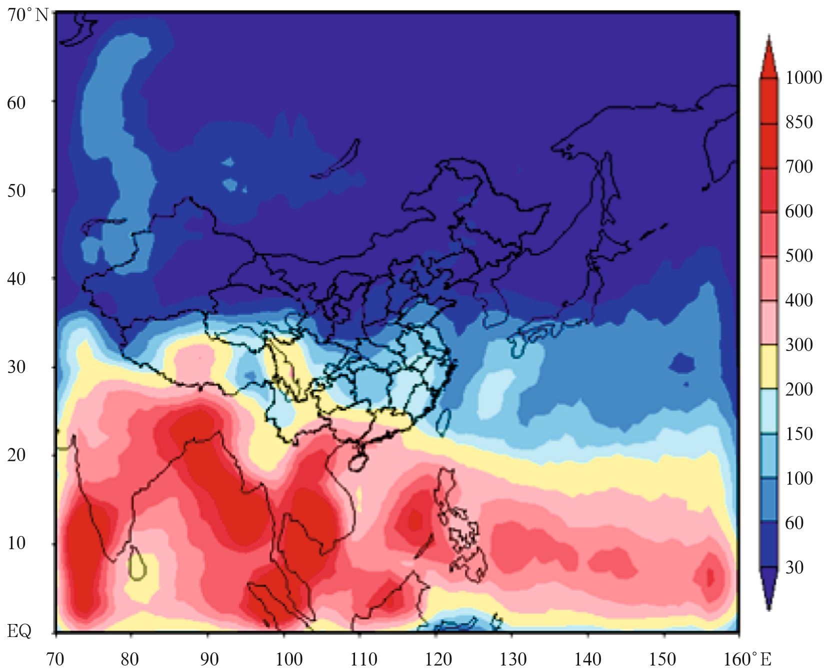

Fig. 1. Geographical distribution of all MCSs during May–October of 1995–2008. The shading denotes the number of MCSs, which is counted in 5°×5° rectangular boxes centered at the corresponding grid points. MCSs are counted according to their maturing positions.

gan Mountains. These MCSs are basically related to some high latitude weather systems such as trough of a low pressure system, front, and so on.

As far as the mainland China is concerned, MCSs occur most frequently over the central Tibetan Plateau. Zhang et al. (2008) pointed out that, in China, hail frequency is also the highest over the central Tibetan Plateau. Though hail seldom occurs in MCSs, they are both intense convective activities. The above conclusions indicate that the central Tibetan Plateau is really favorable for intense convective activities.

4. Diurnal cycles

4.1 Diurnal cycles over the whole region

To study the diurnal cycles of the four MCS types defined in Table 1, the frequency distribution of each type is plotted at each time (figure omitted). The results show that diurnal cycles of the four MCS types are similar on the whole. That is to say, the diurnal cycle of MCSs has little to do with MCSs' shape or size. Hence, in the following, to study the diurnal cycles of MCSs in each area, all MCSs are used as samples. However, because of the special geographical or climatic environment, diurnal cycles of MCSs over different areas differ. Figure 2 gives the frequency distributions of all MCSs at each time.

Figure 2 shows that over the Indian Peninsula, the MCSs are active during 1200–2100 UTC, i.e., from afternoon to midnight. The MCSs over the Bay of Bengal are most active during 2100–0000 UTC, and second active during 0600–0900 UTC, i.e., there are two peaks of MCS activities: the first peak is in the latter half of the night, and the second is in the afternoon. Our results are in agreement with Romatschke et al. (2010) who pointed out that in the South Asian region, extreme convections over the India Peninsula tend to form in the afternoon; but the extreme convections over the Bay of Bengal mainly form after midnight, with afternoon coming next. Moreover, the MCSs over the Indus River Plain and the South China Sea are active all day long, and have almost the same frequency at each time of the day. In the Indochina Peninsula, the MCSs form before 0900 UTC (afternoon), mature at about 1200 UTC (nightfall), weaken during 1500–2100 UTC (midnight), and dissipate during 2100–0000 UTC (next early morning). However, to the east of

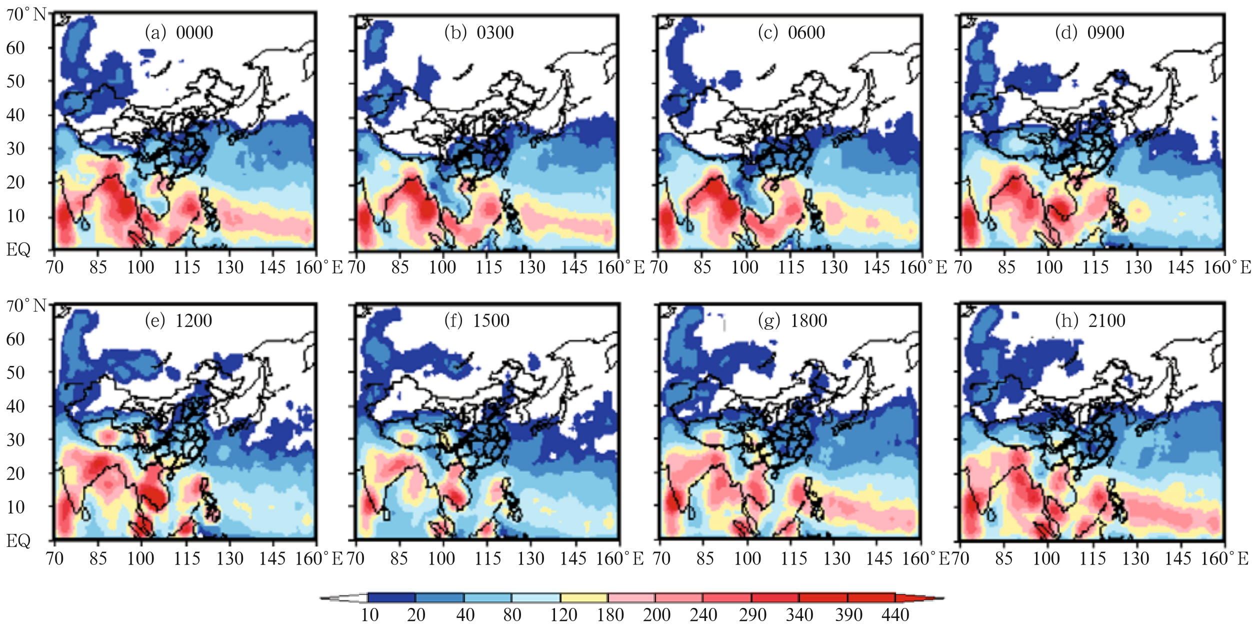

Fig. 2. Geographical distributions of all MCSs at (a) 0000, (b) 0300, (c) 0600, (d) 0900, (e) 1200, (f) 1500, (g) 1800, and (h) 2100 UTC. Other specifications are the same as in Fig. 1.

the Philippines, the MCS diurnal cycle exhibits another kind. They are nocturnal. The MCSs over there form at about 1500–1800 UTC (midnight), mature during 2100–0000 UTC (next early morning), weaken during 0000–0600 UTC (daytime), and dissipate at about 0600–0900 UTC (afternoon).

For the midlatitude zone, the MCSs over the Tibetan Plateau, Hengduan Mountains, and Yungui Plateau form mainly during 0600–0900 UTC (afternoon), mature during 1200–1800 UTC (the first half of the night), weaken and dissipate during the latter half of the night. The MCSs with this kind of lifecycle belong to the typical thermal convections. The MCSs over East China and the coastal area of South China are most active during 0900–1200 UTC (afternoon to nightfall), and most inactive during 2100–0300 UTC (morning). Affected by mountain-valley breeze circulation, the MCSs over the Sichuan basin (including northern Guizhou Province) occur nocturnally. They are most active during 1800–2100 UTC (night). Zhang et al. (2008) indicated that the hail frequency in the Sichuan basin and Guizhou is the highest at night, which agrees with the present work.

In high latitude, the MCSs are inactive all day long. The MCSs over the comparatively active regions, such as the central part of the West Siberian Plain, and Lake Balkhash and Lake Issyk-Kul areas, have almost the same frequency at each time of the day.

4.2 Diurnal cycles along meridian lines

To study the MCS diurnal variations over different areas in detail, the time-latitude (longitude) cross-sections of MCS frequency (Figs. 3 and 4) are plotted along different meridians and parallels. The cross-sections along 75°, 90°, 105°, 120°, 135°, and 150°E are given in Figs. 3a–3f, respectively. Figures 4a–4c give the cross-sections along 10°, 20°, and 30°N, respectively. Figure 3 will be analyzed in this subsection, and Fig. 4 will be analyzed in the next subsection.

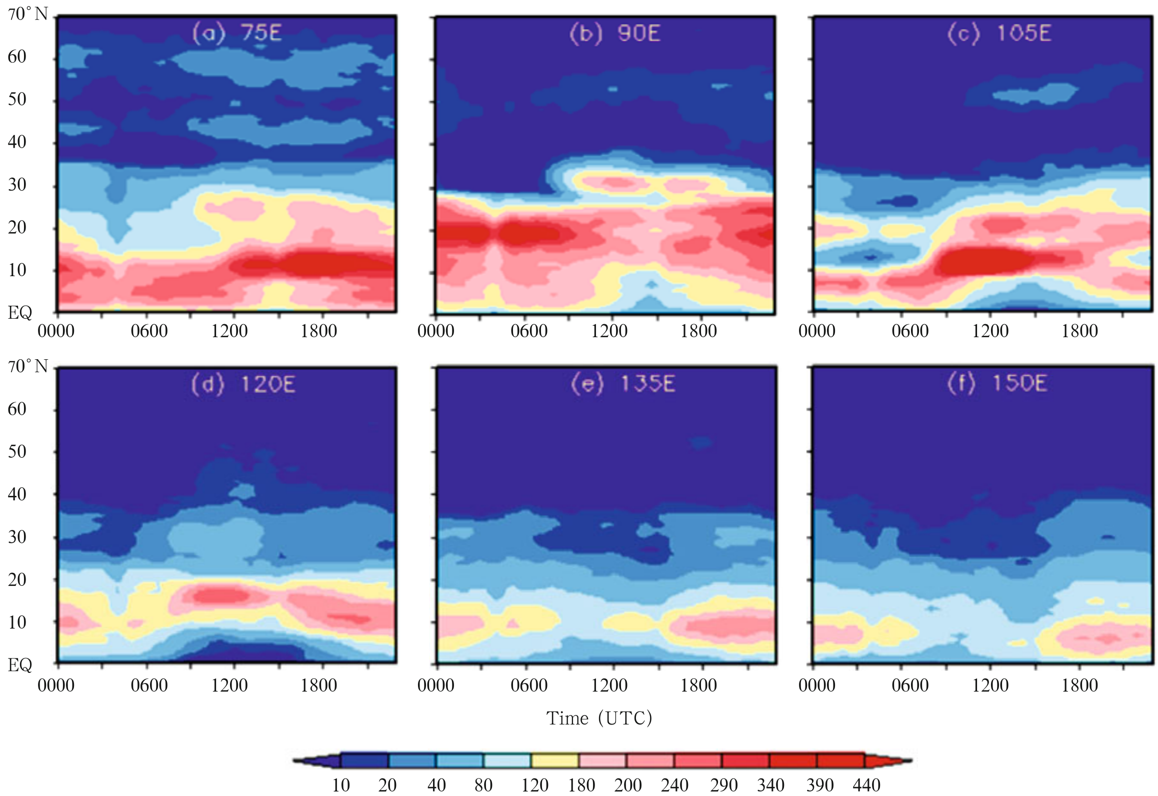

Fig. 3. Time-latitude cross-sections of MCS frequency along (a) 75°E, (b) 90°E, (c) 105°E, (d) 120°E, (e) 135°E, and (f) 150°E. The abscissa axis is time (UTC). Other specifications are the same as in Fig. 1.

From south to north, the 75°E meridian passes through the vicinity of the Maldive Islands, Deccan Plateau, Marwa Plateau, and the central part of the West Siberian Plain. Figure 3a shows that the MCSs near the Maldive Islands (south of 12°N) are active all day long, and they are more active during 1200–0000 UTC within 8°–12°N. The MCSs over the Deccan Plateau and Marwa Plateau concentrate between 1100 and 0000 UTC (afternoon to the latter half of the night). In the central part of the West Siberian Plain (about 60°N), the MCS frequencies are nearly the same at each time of the day.

From south to north, the 90°E meridian passes through the Bay of Bengal, Tibetan Plateau, and Sayan Mountains. The MCSs over the Bay of Bengal (10°–22°N) have two life cycle peaks at 0001 (early morning) and 0700 (afternoon) UTC (Fig. 3b). The MCSs over there concentrate during 2100–0300 and 0500–0900 UTC, i.e., a majority of them are nocturnal MCSs and most of the rest are afternoon MCSs. Besides, it is noticed in Fig. 3b that almost all MCSs over the Tibetan Plateau (30°–37°N) concentrate between 0800 and 2000 UTC (afternoon–midnight). These MCSs are typical thermal convections. They form in the afternoon and dissipate in the first half of the night. There are some MCS activities over the Sayan Mountains (around 50°N), and these MCSs have similar frequency at each time of the day.

From south to north, the 105°E meridian passes through oceans to the east of the Malay Peninsula, Indochina Peninsula, Yungui Plateau, Sichuan basin, Loess Plateau, Mongolian Plateau, and Lake Baikal. Figure 3c indicates that there are two obvious boundaries at 10° and 18°N, which reflect the influence of the underlying surface on the MCS diurnal cycle. The MCSs over the oceans to the east of the Malay Peninsula (south of 10°N) concentrate between 1900 and 0900 UTC (midnight to next afternoon), and there are two peaks at 0100 and 0700 UTC. This diurnal variation is similar to that of the MCSs over the Bay of Bengal. Oppositely, the MCSs over the plain areas of southern Indochina Peninsula (10°–18°N) persist mainly during 0800–1800 UTC (afternoon to midnight), while the MCSs over the mountain areas of northern Indochina Peninsula (18°–23°N) and Yungui Plateau (23°–28°N) mainly occur during 1000–2300 UTC (afternoon to the next early morning). They are postmeridian MCSs. In addition, the MCSs over the Sichuan basin (28°–32°N) are nocturnal, and they concentrate between 1800 and 2300 UTC (the latter half of the night). There are few MCSs to the north of 35°N except the Lake Baikal region. The MCSs over the Lake Baikal region occur during 1200–1800 UTC (the first half of the night).

Figure 3d indicates that, along the 120°E meridian, the MCSs south of 11°N are nocturnal, and they concentrate during 1600–0200 UTC. The MCSs over the South China Sea (11°–21°N) are active at each time of the day. It is noteworthy that, in the plain areas of eastern China, the MCSs have a peak frequency during 0800–1300 UTC (afternoon to nightfall).

In addition, Fig. 3e indicates that, the MCSs near the Caroline Islands (8°–12°N) and Ryukyu Islands (25°–32°N) are nocturnal, and concentrate during 1500–0300 UTC (midnight to noon). Figure 3f shows a similar pattern to Fig. 3e. Along 150°E, the MCSs over the oceans near 10°N and east of Japan are both nocturnal, and they form around 1500 UTC (midnight).

4.3 Diurnal cycles along latitudes

Figure 4a shows the MCS diurnal cycle along 10°N. From west to east, it passes through the Amindivi and Laccadive Islands, Bay of Bengal, Gulf of Thailand, South China Sea, and oceans east of the Philippines. There are two obvious characteristics in Fig. 4a. First, the MCSs over the Amindivi and Laccadive Islands regions (70°–75°E) and over the Gulf of Thailand (100°–105°E) are active all day long, and have nearly the same frequency at each time of the day. Second, along 10°N, the MCSs over other areas concentrate mainly during 1700–1100 UTC. There are two frequency peaks at 0100 UTC (early morning) and 0700 UTC (afternoon). The afternoon peak is obvious to the west of 120°E and inconspicuous to the east of 120°E. This implies that, along 10°N, there are two MCS types to the west of 120°E: the nocturnal MCS and the afternoon MCS; while MCSs to the east of

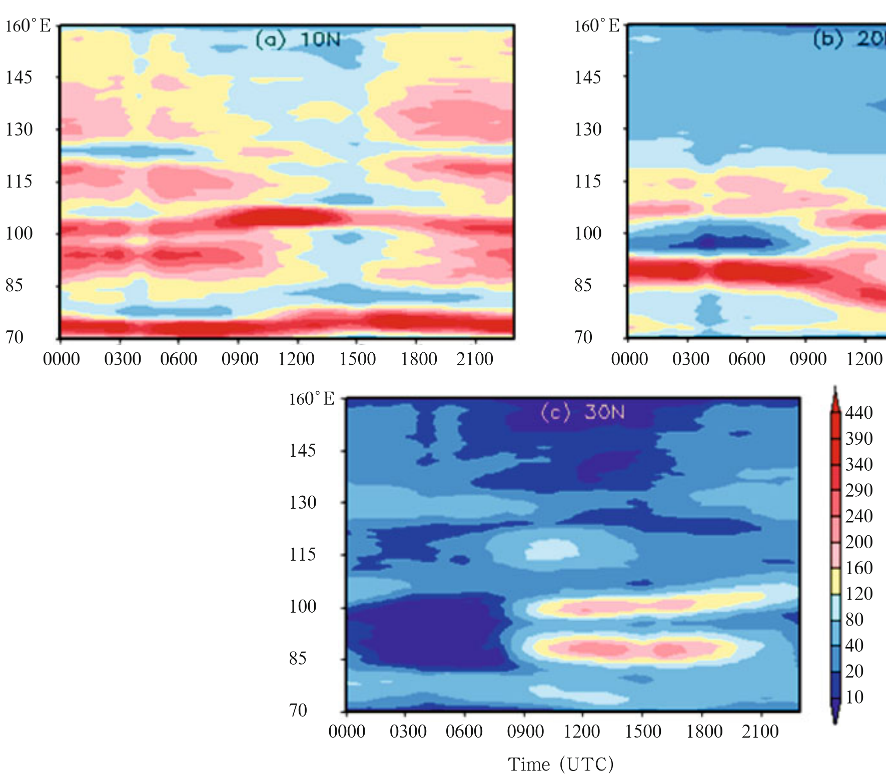

Fig. 4. Time-longitude cross-sections of MCS frequency along (a) 10°N, (b) 20°N, and (c) 30°N. Other specifications are the same as in Fig. 1.

120°E are mainly nocturnal. Sui et al. (1997a) studied the diurnal variations of cumulus convection over the equatorial Pacific warm pool region, and pointed out that there were two convection peaks in the early morning and afternoon respectively. Sui et al. (1997a, b) indicated that the reason for the high convection frequency over oceans at night was the comparatively high humidity and radiative cooling.

From west to east, the 20°N parallel passes through the Deccan Plateau, northern areas of the Bay of Bengal, northern areas of the Indochina Peninsula, and northern areas of the South China Sea. As seen in Fig. 4b, the MCSs over the Deccan Plateau (73°–85°E) and the northern areas of the Indochina Peninsula (100°–106°E) are postmeridian MCSs, and they concentrate during 0900–2300 UTC. The MCSs over the northern areas of the Bay of Bengal (85°–93°E) are nocturnal MCSs. They concentrate during 1900–0900 UTC (midnight to afternoon). As far as the MCSs over the northern areas of the South China Sea (106°–115°E) are concerned, they are active during 0000–0900 UTC (early morning to afternoon). That is to say, these MCSs initiate in the latter half of the night.

From west to east, the 30°N parallel passes through the Indus River Plain, Tibetan Plateau, Sichuan basin, mid-lower reaches of the Yangtze River, and Ryukyu Islands. Figure 4c shows that the MCSs over the Indus River Plain (70°–81°E) occur all the time of the day, and have a weak peak during 0900–1400 UTC (afternoon). It is eye-catching that the MCSs over the central Tibetan Plateau (83°–92°E) are concentrated during 0900–2000 UTC (afternoon to midnight). This is in agreement with the analysis above. Between 92°E and 96°E of the Tibetan Plateau, there are fewer MCSs. The diurnal cycle of the MCSs over the eastern Tibetan Plateau (96°–102°E) is similar to that of the MCSs over the central Tibetan Plateau, but these MCSs have a longer duration: they can last from 0900 to 2200 UTC. Furthermore, affected by the mountain-valley breeze circulation, the active region of MCSs shifts eastward from the plateau to the Sichuan basin (102°–106°E) at about 1800 UTC (midnight). Once again, the MCSs over the Sichuan basin are found to be nocturnal. Their active period is 1800–2300 UTC. In the mid-lower reaches of the Yangtze River (110°–120°E), where mountain and plain alternate, the MCS frequency peaks during 0900–1200 UTC (nightfall), and the convective systems form mostly in the afternoon. The MCSs near the Ryukyu Islands are partly nocturnal. They tend to form at about 1800 UTC (the latter half of the night), and dissipate at about 0900 UTC (nightfall).

4.4 MCS classification

In the above three subsections, we analyze the MCS diurnal cycles in different areas in Asia and the western Pacific region. Generally, we find that the MCS diurnal variation is related to both the large-scale circulation and the local circulation. MCSs in different places have their own special diurnal cycles. Accordingly, MCSs can be classified into four categories: the whole-day occurring MCSs in low latitude, the whole-day occurring MCSs in high latitude, the nocturnal MCSs, and the postmeridian MCSs.

The whole-day occurring MCSs in low latitude are related to favorable convective conditions. The representative areas include the Amindivi, Laccadive, and Maldive Islands, Indus River Plain, Gulf of Thailand, and the South China Sea. The whole-day occurring MCSs in high latitude are related to the high latitude weather systems, such as trough of pressure, cold front, and so on. The representative areas include the central part of the West Siberian Plain, and the Lake Balkhash and Lake Issyk-Kul areas. MCSs of these two categories have nearly the same occurring frequency at each time of the day. However, the whole-day occurring MCS in low latitude is active while the whole-day occurring MCS in high latitude is inactive. The nocturnal MCSs are related to favorable convective conditions at night, such as the comparatively high humidity and radiative cooling over the oceans (Sui et al., 1997a, b), and the upward motions in the basin (Xue et al., 2012). The representative areas include the Bay of Bengal, oceans near Spratly Islands, oceans to the east of the Malay Peninsula, the northern areas of South China Sea, oceans to the east of Philippines, Ryukyu Islands, oceans to the east of Japan, Sichuan basin, and Lake Baikal areas. The postmeridian MCSs mostly take place over plateaus and plains. The thermal effect plays an important role in the formation process of these MCSs. The representative areas include the Tibetan Plateau, Yungui Plateau, Deccan Plateau, Marwa Plateau, Indochina Peninsula, and the area east of China.

In summary, the classification of MCSs over AWPR is shown in Fig. 5. It is noteworthy that such MCS categories occupy a large portion of the MCSs in this region, but not the whole.

5. Summary and conclusion

This study employs the automatic MCS identification method to identify MCSs from satellite infrared imagery. A total of 9241 MαCCSs, 3981 MβCCSs, 25126 MαECSs, and 9120 MβECSs are found over Asia and the western Pacific region during the warm seasons of 1995–2008.

Analysis of geographical distribution of MCSs shows that the MCS geographical distribution has little to do with MCSs' size or shape, and is affected by both the climatic environment and the local circulation. In AWPR, latitude is the primary control factor for the MCS distribution. MCSs are zonally distributed, with three zonations weakening from south to north. The low latitude zone is mainly related to the ITCZ. The midlatitude zone is related to the summer monsoon, and the high latitude zone is related to the high latitude weather systems.

Analysis of diurnal variations of MCSs shows that the MCS diurnal variation has little to do with MCSs' size or shape; MCSs in different areas have their own particular diurnal variation features. Accordingly, MCSs are classified into four categories: the whole-day occurring MCSs in low latitude, the whole-day occurring MCSs in high latitude, the nocturnal MCSs, and the postmeridian MCSs. The nocturnal MCSs are related to favorable convective conditions at night, such as the comparatively high humidity and radiative cooling over the oceans, and the upward motions over the basin at night. The postmeridian MCSs take place

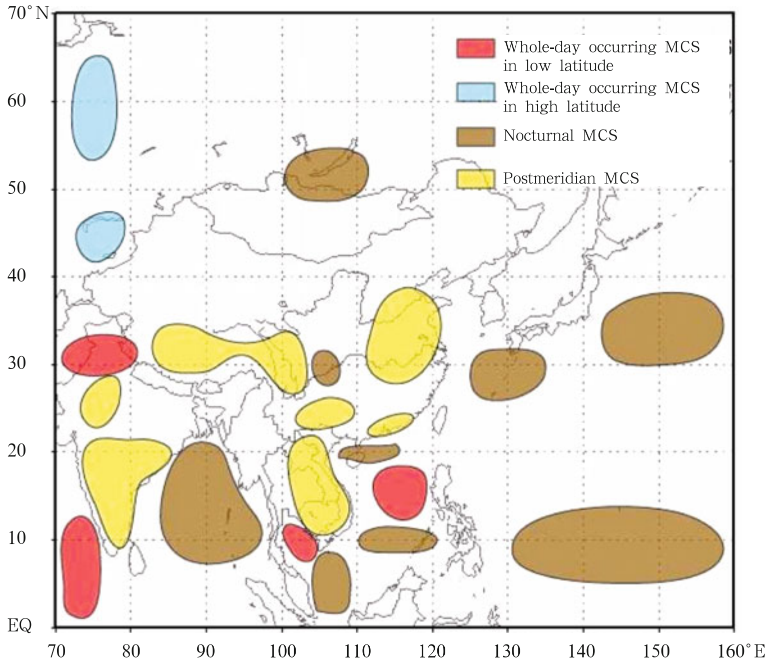

Fig. 5. Classification of MCS diurnal cycles in Asia and the western Pacific region.

over plateaus and plains. The thermal effect plays an important role in the formation of these MCSs.

Compared with past studies on hail and extreme convection (Zhang et al., 2008; Romatschke et al., 2010; Zheng et al., 2008), this study has obtained some consistent conclusions. For example, the central Tibetan Plateau has both the highest MCS frequency and the highest hail frequency; severe convections over the Indian Peninsula and the Bay of Bengal tend to occur in the afternoon and in the evening, respectively; MCSs and hail occur mainly in the afternoon in most of mainland China except in the Sichuan basin and its vicinity, where MCSs and hail often occur during nighttime. These consistent conclusions kind of support the reliability of the present work. Different from past studies, this study employs a new automatic MCS identification method, which is more objective, accurate, and time-saving. On this basis, we have analyzed the diurnal variations of MCSs over Asia and the western Pacific region and found that there are four diurnal cycle categories of MCSs in the study area. In the future, we will make climatic studies of MCSs over other regions by means of the automatic MCS identification method.

Acknowledgments. The authors wish to thank the Atmospheric Department of Kochi University for providing the infrared satellite numerical data.

REFERENCES

Anderson, C. J., and R. W. Arritt, 1998: Mesoscale convective complexes and persistent elongated convective systems over the United States during 1992 and 1993. *Mon. Wea. Rev.*, **126**(3), 578–599.

Augustine, J. A., and K. W. Howard, 1988: Mesoscale convective complexes over the United States during 1985. *Mon. Wea. Rev.*, **116**(3), 685–701.

——, and ——, 1991: Mesoscale convective complexes over the United States during 1986 and 1987. *Mon. Wea. Rev.*, **119**(7), 1575–1589.

Fritsch, J. M., R. J. Kane, and C. R. Chelius, 1986: The contribution of mesoscale convective weather systems to the warm-season precipitation in the United States. *J. Climate Appl. Meteor.*, **25**(10), 1333–1345.

Houze, R. A. Jr., B. F. Smull, and P. Dodge, 1990: Mesoscale organization of springtime rainstorms in Oklahoma. *Mon. Wea. Rev.*, **118**(3), 613–654.

Jirak, I. L., W. R. Cotton, and R. L. Mcanelly, 2003: Satellite and radar survey of mesoscale convective system development. *Mon. Wea. Rev.*, **131**(10), 2428–2449.

Laing, A. G., and J. M. Fritsch, 1993a: Mesoscale convective complexes over the Indian monsoon region. *J. Climate*, **6**(5), 911–919.

——, and ——, 1993b: Mesoscale convective complexes in Africa. *Mon. Wea. Rev.*, **121**(8), 2254–2263.

Lu Xinyan and Duan Yihong, 2011: Characteristics of the tropical cyclogenesis in the summer monsoon trough. *Acta Meteor. Sinica*, **69**(6), 990–1000. (in Chinese)

Ma Yu, Wang Xu, and Tao Zuyu, 1997: Geographic distribution and life cycle of mesoscale convective system in China and its vicinity. *Prog. Nat. Sci.*, **7**(6), 701–706. (in Chinese)

Maddox, R. A., 1980: Mesoscale convective complexes. *Bull. Amer. Meteor. Soc.*, **61**(11), 1374–1387.

——, D. M. Rogers, and K. W. Howard, 1982: Mesoscale convective complexes over the United States during 1981—Annual summary. *Mon. Wea. Rev.*, **110**(10), 1501–1514.

Miller, D., and J. M. Fritsch, 1991: Mesoscale convective complexes in the western Pacific region. *Mon. Wea. Rev.*, **119**(12), 2978–2992.

Parker, M. D., and R. H. Johnson, 2000: Organizational modes of midlatitude mesoscale convective systems. *Mon. Wea. Rev.*, **128**(10), 3413–3436.

Rafiuddin, M., H. Uyeda, and M. N. Islam, 2010: Characteristics of monsoon precipitation systems in and around Bangladesh. *Int. J. Climatol.*, **30**(7), 1042–1055.

Romatschke, U., and R. A. Houze Jr., 2010: Extreme summer convection in South America. *J. Climate*, **23**(14), 3761–3791.

——, and ——, 2011a: Characteristics of precipitating convective systems in the South Asian monsoon. *J. Hydrometeor.*, **12**(1), 3–26.

——, and ——, 2011b: Characteristics of precipitating convective systems in the premonsoon season of South Asia. *J. Hydrometeor.*, **12**(2), 157–180.

——, S. Medina, and R. A. Houze Jr., 2010: Regional, seasonal, and diurnal variations of extreme convection in the South Asian region. *J. Climate*, **23**(2), 419–439.

Roy Bhowmik, S. K., S. Sen Roy, and P. K. Kundu, 2008: Analysis of large-scale conditions associated with convection over the Indian monsoon region. *Int. J. Climatol.*, **28**(6), 797–821.

Shu Yu and Pan Yinong, 2010: Self-identification of mesoscale convective system from satellite infrared imagery. *J. Nanjing Univ. (Nat. Sci.)*, **46**(3), 337–348. (in Chinese)

——, ——, and Wang Wei, 2012: Statistic characteristics of MCSs over Asia and western Pacific region. *J. Trop. Meteor.*, **18**(4), 457–472.

Sui, C. H., K. M. Lau, Y. N. Takayabu, et al., 1997a: Diurnal variations in tropical oceanic cumulus convection during TOGA COARE. *J. Atmos. Sci.*, **54**(5), 639–655.

——, X. F. Li, K. M. Lau, et al., 1997b: Multiscale air-sea interactions during TOGA COARE. *Mon. Wea. Rev.*, **125**(4), 448–462.

Velasco, L., and J. M. Fritsch, 1987: Mesoscale convective complexes in the Americas. *J. Geophys. Res.*, **192**(D8), 9591–9613.

Xue Yujun, Bai Aijuan, and Li Dian, 2012: Analysis and numerical simulation of diurnal variation of precipitation in Sichuan basin. *Adv. Earth Sci.*, **27**(8), 885–894. (in Chinese)

Zhang, C. X., Q. H. Zhang, and Y. Q. Wang, 2008: Climatology of hail in China: 1961–2005. *J. Appl. Meteor. Climatol.*, **47**(3), 795–804.

Zheng Yongguang, Chen Jiong, and Zhu Peijun, 2008: Distribution and diurnal variation of MCSs over China and its vicinity in summer. *Chinese Sci. Bull.*, **53**(4), 471–481. (in Chinese)